EVS24
Stavanger, Norway, May 13-16, 2009

Demonstration of Boost Phase Control Algorithm

John Kajs[1], Dr. Peter Mongeau[2], Dr. Terence Burke[3], Ghassan Khalil[3], Byron Wong[3]
[1]*SAIC, 8303 N. Mopac Suite B-450, Austin, TX, 78758, kajsj@saic.com*
[2]*ePower, Westborough, MA,* [3]*TARDEC, Warren MI*

Abstract

Under the US Army TARDEC Power & Energy program a different control algorithm is being tested for hard switched permanent magnet machine power conversion. This control algorithm can be substituted in place of the more conventional boost PWM algorithm to reduce losses in both the inverter and the machine where applicable. Boost phase control (BPC) reduces the switching frequency of the hard switched inverter to the fundamental frequency of the machine and results in similar frequency content to the machine as SCR or diode rectified but can operate in the region where boosting is required for generator operation and can also be applied in motoring operation. Since the algorithm is implemented with the conventional IGBT/diode hard switched inverter hardware, it is possible to gate the IGBT's and 'boost' the AC voltage of the machine. This boosting functionality allows a PM generator to provide power to a DC bus even when the line to line open circuit voltage of the machine is below the DC bus voltage similar to boost PWM, however with significantly lower switching losses. At the same time as the switching losses are lower for the inverter because of the reduced switching losses, the machine losses can be lower over some operating regions.

This paper reports the experimental comparison of the results measured with the same hardware for both hard switched PWM and boost phase control. Experimental results are reported for testing from 1500 to 2500 RPM at power levels appropriate for the hardware under test (up to ~100 kW) with both electrical and thermal measurements made to estimate the losses and compare the results.

Keywords: converter, DC-AC, primary energy, synchronous motor, optimization, demonstration

1 Introduction

The US Army TARDEC & Energy program performs research on a number of areas for hybrid electric vehicles. One of the things of interest is efficient and compact power conversion for PM machines to a DC bus. In this case what is being investigated specifically are ways to

efficiently convert power from an engine to a DC bus which allows the engine and generator to operate at it's most efficient fuel consumption point for a given power level. As an example, diesel engines typically have lower fuel consumption for lower power at lower speed and lower fuel consumption at high power at higher speeds. One way this can be accommodated with a constant DC bus voltage and a PM generator is by using a boost rectifier where the open circuit voltage of the generator is lower than the DC bus voltage and then using a PWM converter to control the power flow. Boost phase control (BPC) is a control algorithm that can be used with hard switched PWM hardware that reduces the switching frequency of the hard switched inverter to the fundamental frequency of the machine and results in similar frequency content to the machine as SCR or diode rectified but can operate in the region where boosting is required for generator operation. At the same time as the switching losses are lower for the inverter because of the reduced switching losses, the generator losses can be lowered as a result of lowering the frequency of the harmonics over some operating regions.

This paper reports the experimental comparison of the results measured with the same hardware for both hard switched PWM and boost phase control. Experimental results are reported for testing from 1500 to 2500 RPM at power levels appropriate for the hardware under test (up to ~100 kW) with both electrical and thermal measurements.

2 Algorithm Description

For permanent magnet machines, at the upper end of the speed range, boost inverters operate with phase to phase voltage very near the bus voltage. When this is happening, there can be advantages to going away from boost PWM and dramatically reducing the switching frequency by going to switching algorithms similar to six step regulation. One of the downsides of six step algorithms is that the voltage control is reduced from the two degrees of freedom (amplitude and phase shift between the terminal voltage and back-emf) with Pulse Width Modulation (PWM) to a single degree of freedom with six-step mode (just the phase shift).

Utilizing Boost Phase Control (BPC) with a Y configured electric machine is similar to six-step except that the gating purposely introduces periods where a phase is not actively gated either high or low. This results in a low switching frequency control methodology which has control for both the amplitude and the phase of the terminal voltage allowing operation at lower speeds/terminal voltages than is practical for six step control. Basically, the BPC gating can be defined by a delay angle from when the back-emf changes sign where the IGBT is gated on plus an on duration.

For the current regulation of the inverter in BPC, a simple field oriented control based on the fundamental of the phase currents is feasible. A simple PI feedback control was utilized for this set of tests where the delay angle was corrected based on the observed reactive (or Id) current and the on duration was corrected based on the observed real (or Iq) current. As an example of the algorithm, in Fig. 1 a simplified computer model of the system has been exercised to show the expected waveforms for the test hardware when operating at 1500 RPM, with a 600 Volt bus, a delay of 30 degrees and an on duration of 30 degrees (this is approximately the operating condition for obtaining an Iq of 200 Amps as shown in the test data in Fig. 7). Only one of the 3 phases is shown in Fig. 1 for clarity. The gating signal shown goes to 1 when the positive side IGBT is gated and -1 when the negative side IGBT is gated.

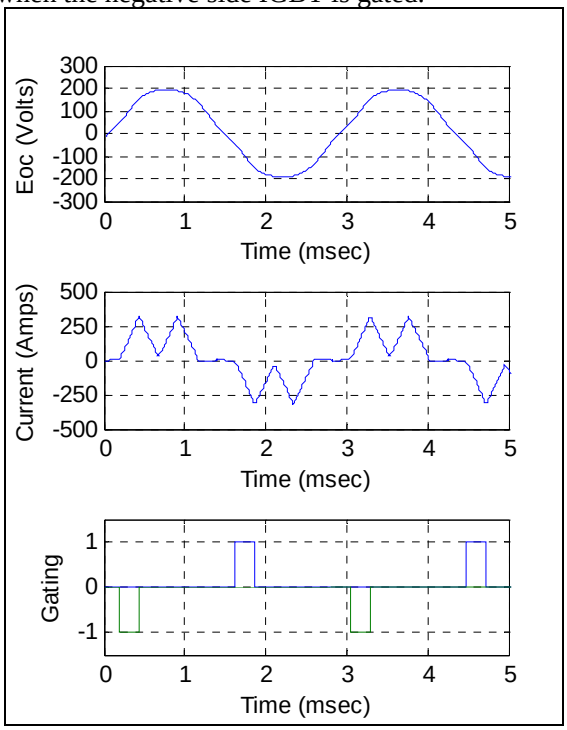

Figure 1. BPC Algorithm Example.

It can be seen in this case, the current is only being carried in the IGBTs for a fairly short fraction of the time and there will be rather low amounts of switching losses in the IGBTs due to the small

number of switching events (once per electrical cycle per IGBT). However, distortion of the phase currents can also be observed which will cause heating in the machine. If the distortion becomes significant, the additional losses could also become significant. Substantial portions of the high frequency losses from this current distortion will typically be on the rotor which often has rather poor cooling mechanisms. As a result of the negative impact on the electric machine thermal management from high frequency currents, in addition to doing a comparison based on inverter losses, machine losses and total losses, the high frequency machine losses will also be compared between PWM and BPC.

3 Basic Approach

The basic test setup was created using a combination of commercial off the shelf (COTS) hardware and existing hardware. The inverters utilized are liquid cooled inverters with the available vendor provided TI ‘2812 motor control DSP board for providing the gating control. The machine is a standard, surface mounted magnet, axial gap PM machine with two sets of windings each connected in a Y connection to their own inverter. There are also some external choke inductors installed between the machine windings and the inverters. These chokes add approximately 50 μH to the 60 μH of the winding inductance of the generator to allow this standard PM machine to be flux weakened and operate adequately from a 600 Vdc bus up to 3300 RPM (without the additional inductance the reactive current for flux weakening at the high speed would become excessive). This machine is a standard PM machine designed to be primarily diode rectified and when operated at the higher speeds was expected to operate from a higher voltage bus (closer to 750 Volts) than the 600 volt bus for the present system.

The coolant flows, inlet and outlet temperatures for both the inverters and machine were instrumented to estimate the heat removed during the tests. Electrical measurements were made with two power analyzers having 100,000 samples per channel and 8 channels per analyzer set to sample at 5 MS/sec. The analyzers have 4 current inputs that were connected with closed loop hall effect current sensors rated for >100 kHz response rate and the 4 voltage inputs were directly connected to the analyzers without external signal conditioners. Measurements were made from all of the points labelled A, B & C to a floating neutral and from P to M for the DC along with the 4 shown currents (Ia, Ib, Ic & Idc). The second power analyzer was connected to measure the external choke inductor response and effects.

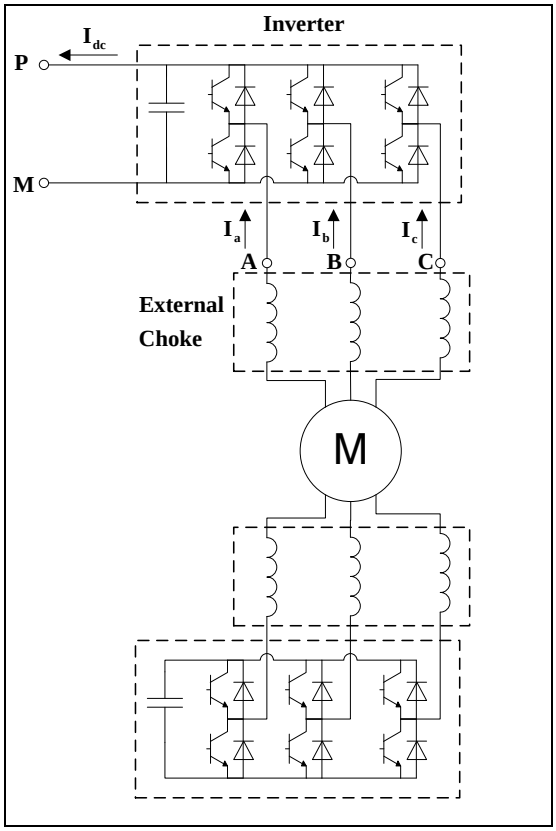

Figure 2. Basic Experimental Setup.

During these tests, only one set of windings and one of the inverters were actually used. In order to go to the full generator and engine ratings without worrying about thermal margins, it is necessary to use both sets of windings and both inverters. In order to simplify things for these tests, only the upper half of the above system was used. Not using this bottom half but still having it connected to the bus (in case of a failure this second inverter would act as a diode rectifier to stop engine runaway), does limit the operation from a 600 volt bus to below ~2500 RPM to avoid currents flowing in this lower inverter from passive diode rectification. To begin investigating the regions where flux weakening is required (above 2500 RPM) will necessitate either completely disconnecting this 2nd inverter or else using both inverters simultaneously. In addition to the above main power system hardware, a simple interface between the resolver coming from the generator to provide angle information to the DSP was created.

Table 1. Nominal Component Parameters

Rated speed	2860 RPM
Rated power at 2860 RPM	336 kW
Machine continuous current	370 Arms
Machine pole pairs	14
Machine winding resistance (per winding)	22 m Ohms
Machine winding inductance (per winding)	60 μH @ 500 Hz
Machine rated coolant temp.	49 C
Machine nominal rated flow	3.5 gpm per stator
Machine # stators	2
Machine Windings per stator	3
Machine Fund Vconst (per winding)	0.16 Vrms, L-L per RPM
Inverter nominal rating	300 Arms
Inverter device voltage rating	1200 Volts
Inverter allowable DC voltage	900 Volts
Inverter max switching Fsw	15 kHz
Inverter nominal coolant temp.	50 C
Inverter nominal coolant flow	2-3 GPM
Nominal Choke Inductance @ 60 Hz	50 μH
Nominal Choke Fund Amps @60 Hz & 45 C Ambient	500 Arms

4 Testing Performed

Two sets of tests were performed with the only difference being the gating algorithm used, one set with the boost phase control (BPC) and the other using 5 kHz hard switched PWM. Both BPC and PWM were operated with field oriented control (FOC) where the fundamental of the currents were kept in phase with the fundamental of the back-emf of the machine to minimize the current required to extract a given power (and thus minimizing the losses for the given gating algorithm). The same FOC calculation routine for estimation of the real (Iq) and reactive (Id) currents was used for both algorithms. A test matrix of desired operating points (speeds and Iq) was created. Speed and power combinations which would require flux weakening were avoided for this round of testing. For the PWM cases, standard FOC techniques adjusting the Vd & Vq commands based on the observed Id & Iq and desired Id and Iq (for these cases Id desired was always zero since there was no flux weakening). For the BPC, at a given speed the observed Iq was compared to the commanded Iq and the gating on time was adjusted to get to the commanded Iq. The delay angle was adjusted based on the observed reactive (Id current) to minimize it. The full test matrix of points tested is shown in Table 2. Other test points are also feasible, but the 12 test points below will be used for most of this paper.

Table 2. Full System Test Matrix.

Speed (RPM)	Iq Commands (Amps Peak)
1500	50, 100, 150 & 200
2000	50, 100, 200 & 300
2500	50, 100, 200 & 300

During the testing, the objective was to stay close to each of these test points for ~5 minutes to allow the liquid cooled inverter to come close to thermal equilibrium and thus to enable estimating the inverter losses from the heat removed from the inverters with the liquid cooling. For this test setup, the inverters are located on their own stand which helps to provide some thermal isolation, though some heat will be removed in other methods than from the measured liquid cooling. However, the exact same thermal measurements were made in both cases, and the tests reported here were all collected on the same day (BPC and PWM). Due to the fact that the generator is in contact with a fairly large area of the engine, there appears to be a large enough fraction of the heat from the generator that is removed by other mechanisms than the generator liquid cooling and also that some of the engine heat is removed by the generator cooling making the thermal measurements from the generator un-useable for generator loss estimates.

4.1 Inductor Test Results

The inductors inserted between the inverter and generator are designed primarily for 60 Hz operation to reduce the impact of inverter harmonics on machines. However, the manufacturer advertises that they can be used at higher frequencies at reduced current levels, but there is limited manufacturers data (such as losses and inductance) at these higher frequencies. A compilation of power analyzer data measuring just the inductor voltage and currents was performed to estimate the equivalent resistance and inductance at the fundamental frequencies tested for each dataset run.

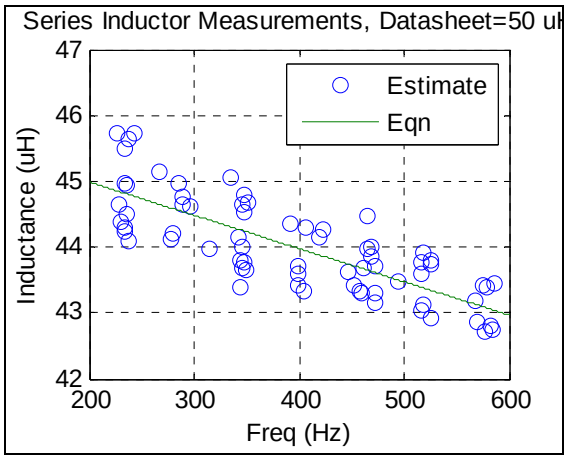

Figure 3. Choke Inductor Inductance.

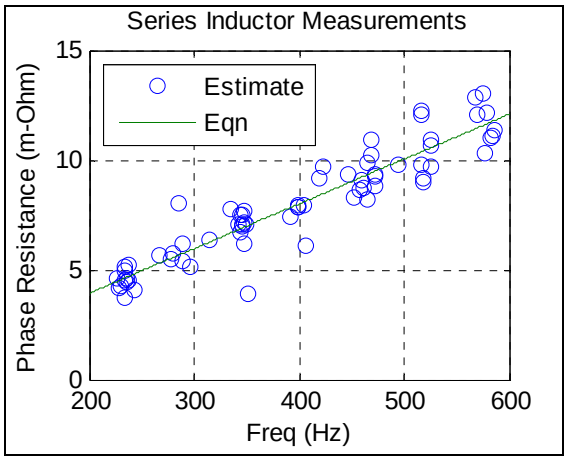

Figure 4. Choke Inductor ESR.

This inductor analysis was done by calculating just a fundamental current and fundamental voltage (complex in both cases) and then doing a simple Z=V/I=R+jωL and plotting vs the fundamental frequency. From this data, it appears that a simple linear curve fit for the inductance vs frequency for up to 600 Hz will give the inductance of the inductor within ~5% ignoring any saturation or current amplitude effects with the inductance. This curve fit would estimate the inductance at 60 Hz of ~46 μH which is ~90% of the datasheet stated inductance value of 50 μH. A linear curve fit for the resistance of the inductors vs frequency appears to be a reasonable fit. This data also indicates that the losses at the fundamental frequencies expected from these inductors should be less than half that to be expected from just the ESR of the machine.

4.2 Inverter Test Results

For the inverter losses the primary method used to estimate the losses was based on the heat removed by the liquid coolant. Because of the relatively short thermal time constant of the inverter (reached reasonable thermal equilibrium after about a minute at an operating point) and the relative thermal isolation of the inverter this is considered to give reasonable values. The exact values of losses from the inverters are not claimed to be highly accurate (probably no closer than 15%). However, since the exact same setup was used for both sets of tests and the tests for the comparisons were performed on the same day with just code changes in the DSP, it is believed the results should be appropriate for relative comparisons between the two gating algorithms.

The power analyzers are continuously run and the data is then post-processed by the power analyzer and a set of overall values (mean Volts & Amps, rms Volts & Amps, AC Power, DC Power etc) are recorded at 2 second intervals for later use. The times when the markers stop temporarily for the DC power (for instance from ~2-3.5 minutes) are times when the full time domain data of 100,000 datapoints for each of the 16 channels of data from the 2 power analyzers are downloaded. The thermal measurements are continually logged and the inverter continues operating during this time. The 'Inverter Losses' are calculated based on the simple equation

$$P = C_p F_{mass} (T_{out} - T_{in}) \qquad (1)$$

using measured flow rates from flow sensors, measured inlet and outlet coolant temperatures from thermocouples which are updated at a 1 Hz rate and typical fluid properties.

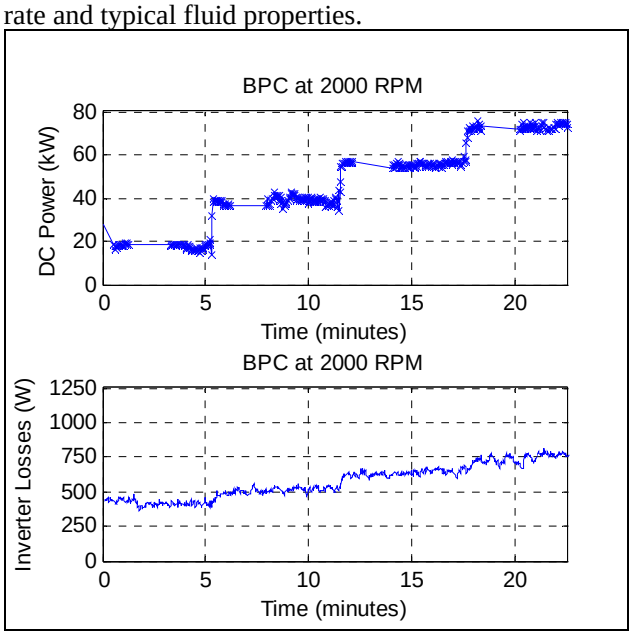

Figure 5. Example BPC Thermal Data.

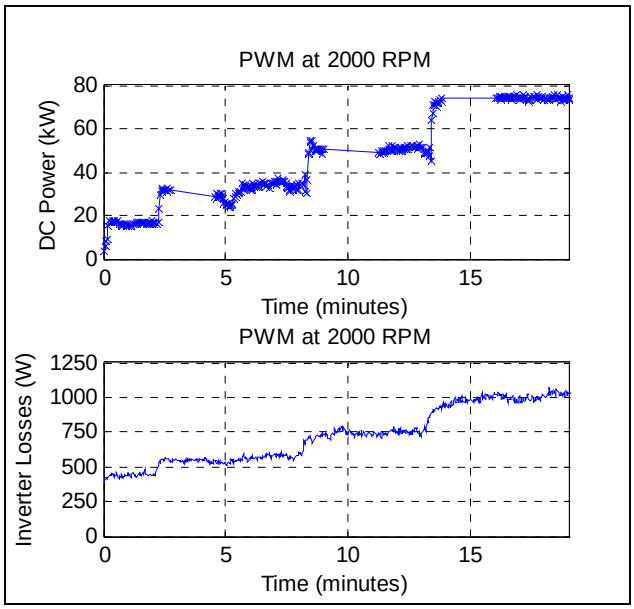

Figure 6. Example PWM Thermal Data

In addition to the thermal estimate of heat removed, the actual operating conditions for the inverters were estimated from the power analyzer time domain data downloaded. This was done by calculating the fundamental (complex quantities including amplitude and phase) for both the voltage and currents from the data (including an estimate of the fundamental frequency). Below are a couple examples typical of the data collected. In the graphs are shown both the measured time domain data along with the estimated fundamental currents and voltages.

The 1st case is at low speed and max torque (1500 RPM, Iq=200, Power~55 kW) where it turns out BPC has lower inverter losses than PWM (~33% lower) due to the reduced switching frequency losses, but due to the waveform distortion, the harmonic losses for the generator and inductors for BPC are estimated at ~2x those of PWM (total losses ~30% higher). The estimated fundamental frequency losses for both algorithms are very close because the field oriented control was able to achieve its objective for both algorithms.

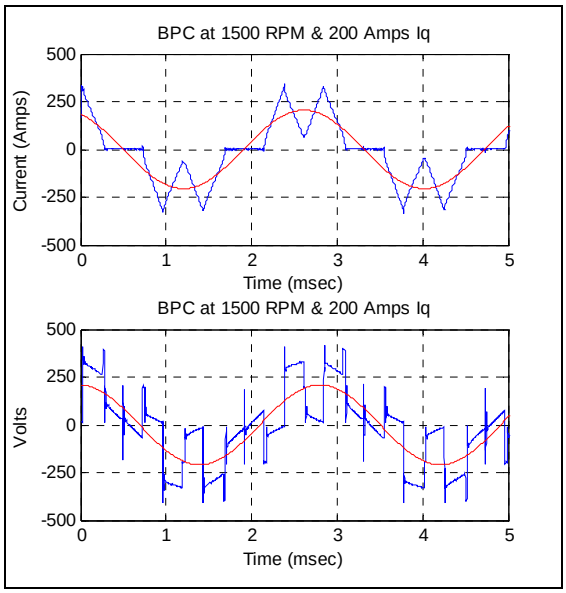

Figure 7. Example BPC Data at Low Speed.

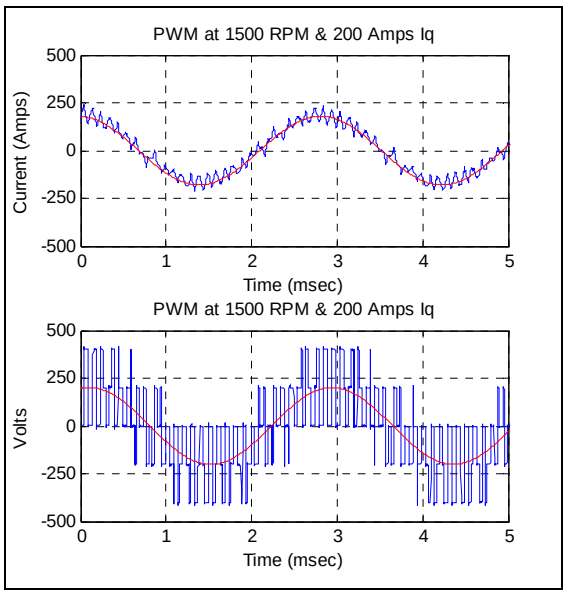

Figure 8. Example PWM Data at Low Speed.

The 2nd case is at high speed and moderate torque (2500 RPM, Iq=150 Amps, Power~70 kW) where it turns out BPC has lower inverter losses than PWM due to the reduced switching frequency losses (~30% lower), but due to the frequency of the waveform distortion, the harmonic losses for the generator and inductors for BPC are estimated lower as well (~33% lower).

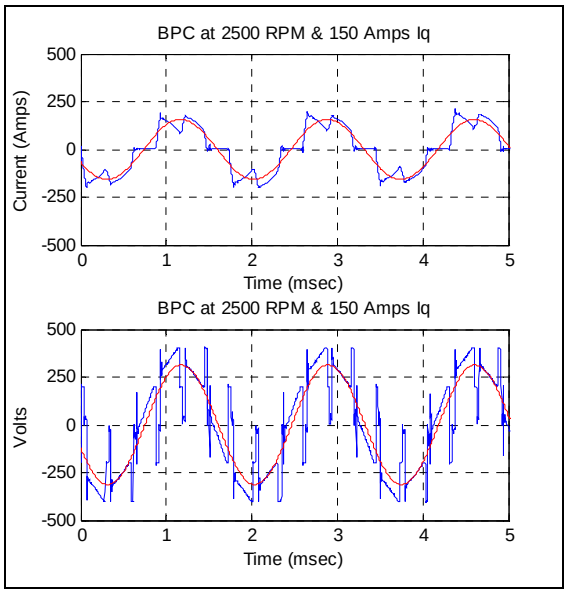

Figure 9. Example BPC Data at High Speed.

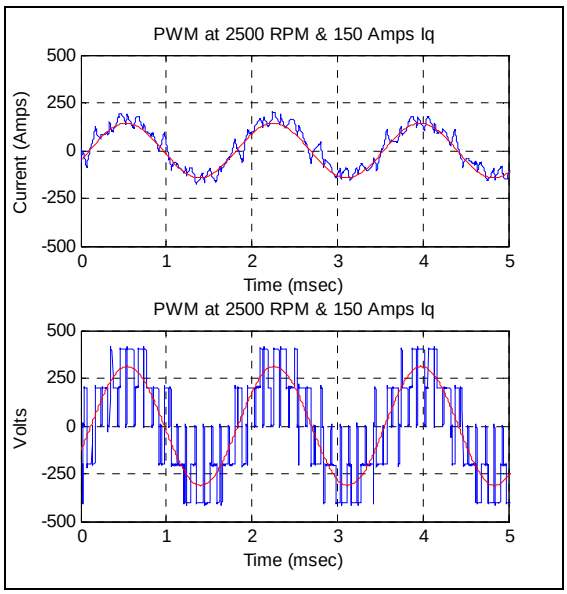

Figure 10. Example PWM Data at High Speed.

4.3 Inverter Loss Validation

With the numbers for the losses in the inverters (as measured from the thermal) being as low as they were (at the top end indicating almost 99% inverter AC/DC efficiency), some validation calculations were performed. The 1st calculation (labelled 'Vendor' in Table 3) was performed using the online tool from the inverter vendor along with the fundamental components estimated for both the AC voltage and currents and the DC components (methodology for estimating fundamental quantities provided in a later section). A loss estimate was calculated using nominal device values provided by the vendor and just the fundamental of the current but using the actual switching waveforms measured (labelled 'Fund' in Table 3). Next, the same calculation was done using the total AC currents and the same estimation routine for the inverter losses (labelled 'Total' in Table 3). The inverter loss estimates used throughout this paper are those estimated from the heat removed from the engine (labelled 'Therm') in Table 3.

Table 3. Inverter Loss Validation Data.

RPM (Meas)	Pdc (kW)	Vendor (W)	Fund (W)	Total (W)	Therm (W)
1500	8.9	164	183	232	382
1500	22.9	372	367	388	568
1520	37.6	600	583	596	748
1510	50.6	834	816	827	987
1980	16.1	222	229	283	437
1987	31.7	382	379	415	572
1987	50.3	602	591	618	751
2019	74.0	900	889	910	1029
2500	20.9	237	226	294	430
2497	43.3	425	403	452	572
2492	66.9	653	627	666	844
2516	94.0	923	896	929	1019

Comparing the loss calculation for just the fundamental of the current but the actual switching waveforms and nominal device parameters agrees within -6% to +11% of the loss estimates provided by the online tool by the inverter vendor. This is considered to be within the accuracy of the calculation method used for the 'Fund' calculation in this case and provides a reasonable validation of the 'Fund' calculation. Including the harmonics of the current (in the 'Total' column) increases the inverter loss estimate by 1.3-30% compared to ignoring the harmonics ('Fund' column). What the calculations show is that the losses in the inverter as estimated by the heat removed from the inverter are between 96-217 Watts higher than the estimates provided by the vendor which don't take into account harmonics of the current. Even though these inverter losses seem low for the operating conditions (inverter efficiencies of ~99% for some tested points), the estimated losses from the thermal measurements are consistent with vendor provided data for these inverters but were always higher (measurements were less efficient than vendor model). The conclusion is that the thermally estimated inverter losses (what is used for comparison in this paper) do seem to be reasonable estimates of the inverter losses.

4.4 Machine Loss Estimate

Because the generator thermal measurements were not useable for estimating generator losses, another method of calculation was necessary. To accomplish this, the data downloaded from the power analyzers was used extensively in combination with post-processing techniques which will be described here.

The first step was to take the AC currents that were measured for each test point and perform an FFT routine on the waveforms. Next a search of the lowest 100 frequency domain values is done to find the approximate fundamental frequency. The FFT frequencies are spaced apart at multiples of the original sample period. Since the time domain data was sampled over 40 msec windows, the frequency increments for the FFT data were effectively 25 Hz or 107 RPM steps. After the approximate fundamental frequency was found from the FFT, an iterative cross correlation was done to estimate the fundamental frequency to less than approximately 1 RPM error shown in the later data. The next step was to perform the FFT algorithm on both the voltage and current data and then scale the data to get volts and amps as a function of frequency. The real power can then be calculated as P=real(V*conj(I)). Finally, the net power out of the machine over a range of frequencies can be done by summing the values over the given frequencies (ignoring any effects of higher frequencies being aliased down).

For illustrative purposes of this frequency domain post-processing, the highest power PWM case will be used. This case was at ~2500 RPM & 94 kW of DC power. According to the frequency iteration, the fundamental frequency is at 587 Hz for this case. Below is plotted the 1st part of the 40 msec measured for both the measured phase A current plus the estimated fundamental current at 587 Hz using the cross-correlation technique. As long as the operating condition doesn't change significantly during the sample window (in this case 40 msec), the agreement throughout the rest of the time period is similar as this section of time.

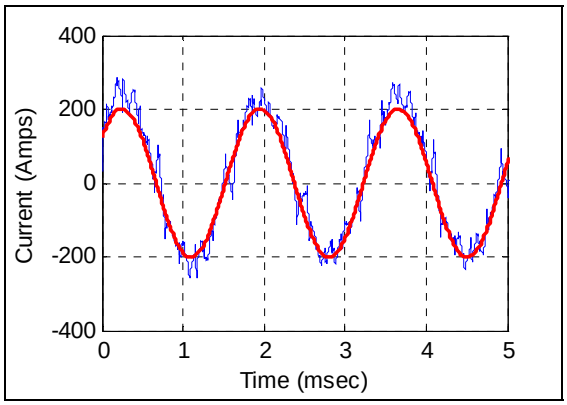

Figure 11. Sampled and Fundamental Current.

Looking at the frequency domain values as returned by the FFT, what is seen is that the 201 Amps of fundamental current at 587 Hz ends up spread over the frequencies around the fundamental frequency since the fundamental frequency was not at a multiple of 25 Hz. This spreading of the amplitudes when the sample period doesn't cover exactly an even multiple of fundamental periods is expected when using an FFT technique.

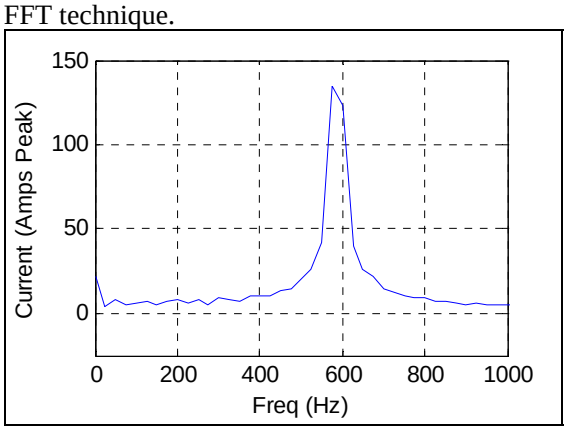

Figure 12. FFT of Sampled Current.

Table 4. Selected Numeric Values from FFT.

Freq (Hz)	Ia (Amps)
525	25.7
550	41.8
575	132.4
600	122.3
625	39.5
650	25.3

Taking the square root of the sum of the squares of the FFT currents close to the fundamental frequency (3 above and 3 below in this case) results in a value very close to the estimated fundamental current from the cross-correlation.

$$I_{fund} \sim \sqrt{\sum I^2} = 193 = 0.96 * 201 \qquad (3)$$

When the lowest frequency of the signals is the fundamental (as is true for these data), to obtain the amplitude of the fundamental, it is also feasible to use equation (3) starting at DC and summing through approximately 1.5 times the fundamental frequency. Performing this calculation for both the voltage and current results in estimated fundamental amplitudes for this dataset of 204 Amps peak and 550 Volts L-L peak. These are within 1.5% of the cross-correlated estimates of 201 Amps and 349 Volts. Looking at the FFT of the voltages, the expected peaks from the FFT are visible around the fundamental (587 Hz) plus the multiples of the switching frequency (5 kHz) plus and minus the appropriate multiples of the fundamental frequency.

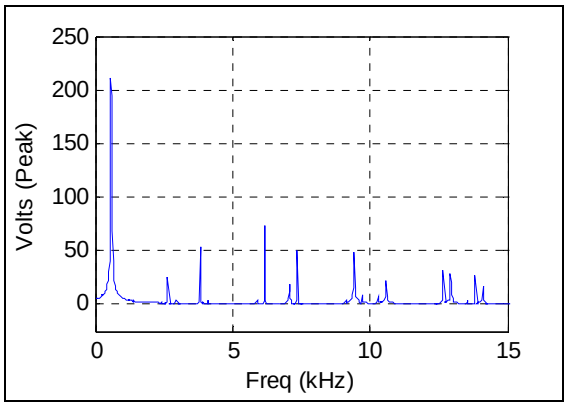

Figure 13. FFT of Voltage (L-N)

With the frequency amplitude of the voltages (L-N) and currents scaled for amplitude peak, the power for each phase in the frequency domain can be calculated using the following equation

$$P=\text{real}(V*\text{conj}(I))/2 \quad (4)$$

Adding the power from all 3 of the phases results in the significant power being positive (generating power) up until the fundamental frequency components are completed after which the power is negative indicating power going back into the machine which are assumed to be losses. In truth, a small fraction of the power at these higher frequencies would be expected to be creating mechanical power similar to an induction machine (both positive and negative) and would not be losses. However, without details about the internal design of the machine it is not practical to try to separate this mechanical power from the losses. In addition, there are always similar amplitude backward rotating harmonics which will result in similar amplitude mechanical power acting as a generator extracting mechanical power, and as a result of the high slips involved (>0.75) the vast majority of the power going into induction motor action would be losses anyway.

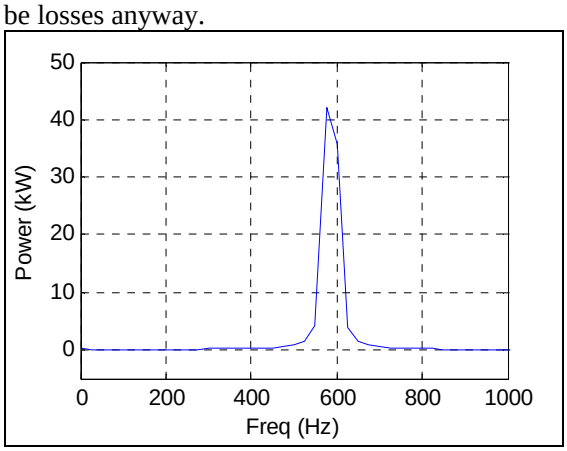

Figure 14. Lower Frequency Power.

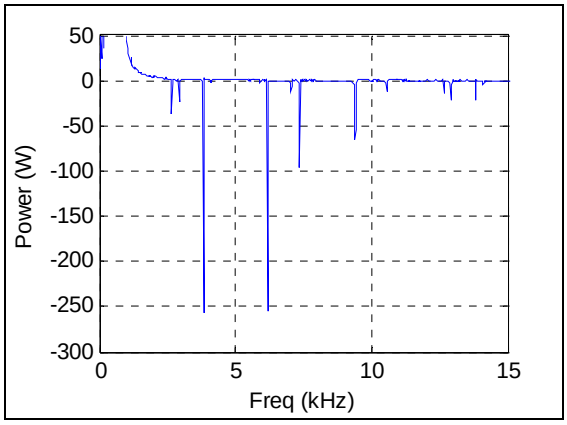

Figure 15. Higher Frequency Power.

As a result of the spreading of the frequencies, one of the more useful things for the power is to calculate a cumulative sum of the power up to each frequency. What is seen is that this cumulative power reaches its maximum at about 2x the fundamental frequency and declines afterward.

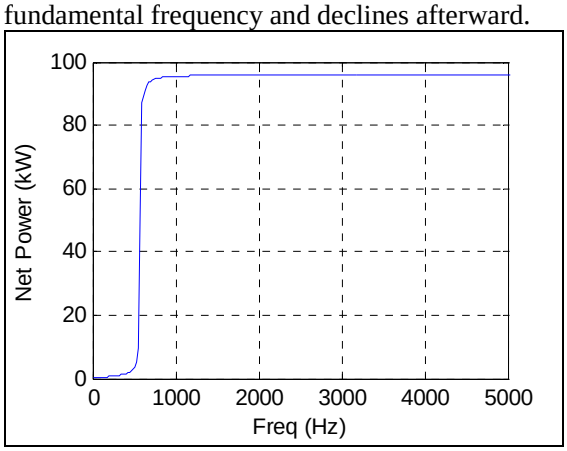

Figure 16. Lower Frequency Net Power.

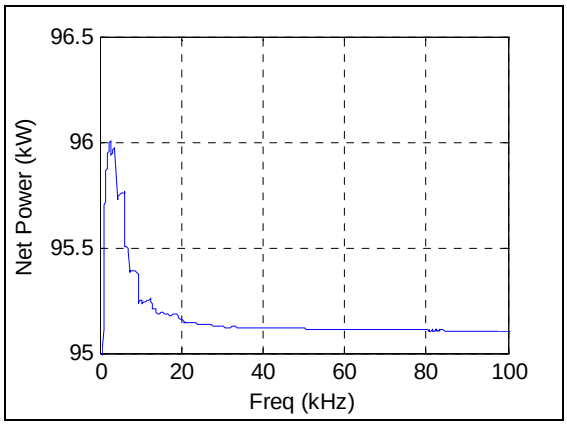

Figure 17. Higher Frequency Net Power.

As a result of the fact this experimental setup, the fundamental power is generating power and negative power is power going into the machine based on the sign conventions chosen for the sensors. To estimate the harmonic losses in the machine, the peak value of the summation of the power shown in Fig 16 & 17 is taken as the net fundamental power being extracted from the machine. The assumption is made that the difference between this fundamental power and the net AC power extracted from the machine is assumed as higher frequency harmonic losses. As described earlier, this does involve some simplifications. However, for the relative comparison between PWM and PBC, this should be accurate enough.

There is still the issue of how to estimate the fundamental frequency losses. Conveniently, fundamental currents for both PWM and BPC were controlled with the same algorithm, thus the fundamental current for each generator torque/speed point were practically identical, thus the fundamental losses end up being also practically identical. Because no information was provided about the core losses in the machine, these have been ignored for the fundamental loss comparison. For the external inductor losses, the fundamental losses in these were estimated by the cumulative sum of the power at 2x the fundamental frequency. For the generator itself, the fundamental losses were estimated using the datasheet ESR value and the measured fundamental current. Once again, since a relative comparison between PWM and BPC is the purpose of this paper, this should be accurate enough.

5 Overall Results

Once the values for both the fundamental and high frequency losses (labelled 'Harm') were estimated, the results could be compared. The overall results for actual power and losses are shown in tables 5 & 6.

Table 5. BPC Power & Losses.

RPM (Meas)	Pdc (kW)	Inv (W)	Fund (W)	Harm (W)	Total (W)
1506	13.6	308	115	769	1192
1500	27.2	483	485	1262	2229
1492	39.9	516	1002	1733	3251
1522	56.1	660	1866	1982	4508
1968	17.9	410	122	511	1042
1969	35.7	526	464	626	1615
2004	56.1	634	1102	867	2602
1996	73.3	771	1933	1421	4124
2493	22.2	416	101	254	771
2530	54.1	455	583	408	1446
2495	71.8	603	1181	687	2472
2485	93.2	722	2019	931	3672

Table 6. PWM Power & Losses.

RPM (Meas)	Pdc (kW)	Inv (W)	Fund (W)	Harm (W)	Total (W)
1500	8.9	382	55.7	990	1428
1500	22.9	568	308.4	994	1870
1520	37.6	748	789	958	2494
1510	50.6	987	1446	1027	3460
1980	16.1	437	98	1065	1601
1987	31.7	572	343	1059	1974
1987	50.3	751	868	1008	2627
2019	74.0	1029	1819	1065	3913
2500	20.9	430	132	915	1477
2497	43.3	572	430	986	1988
2492	66.9	844	1085	1038	2967
2516	94.0	1019	2070	977	4066

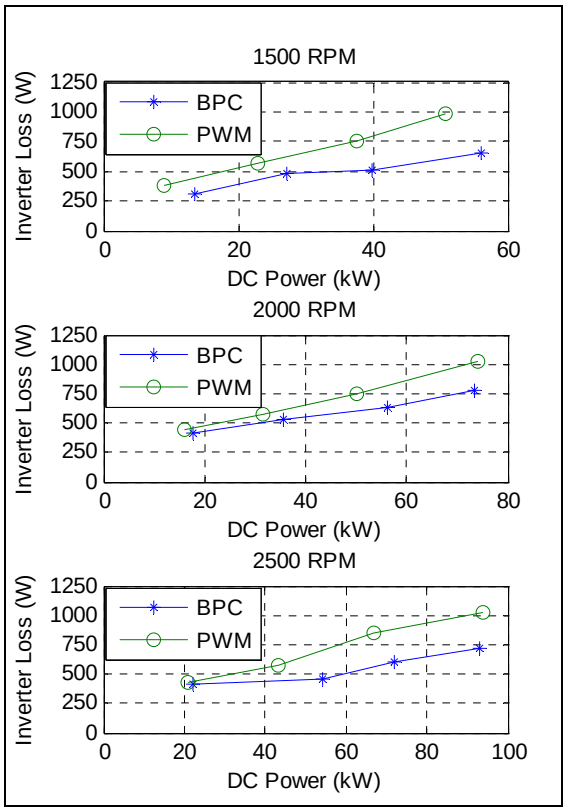

Figure 18. Inverter Loss Plots.

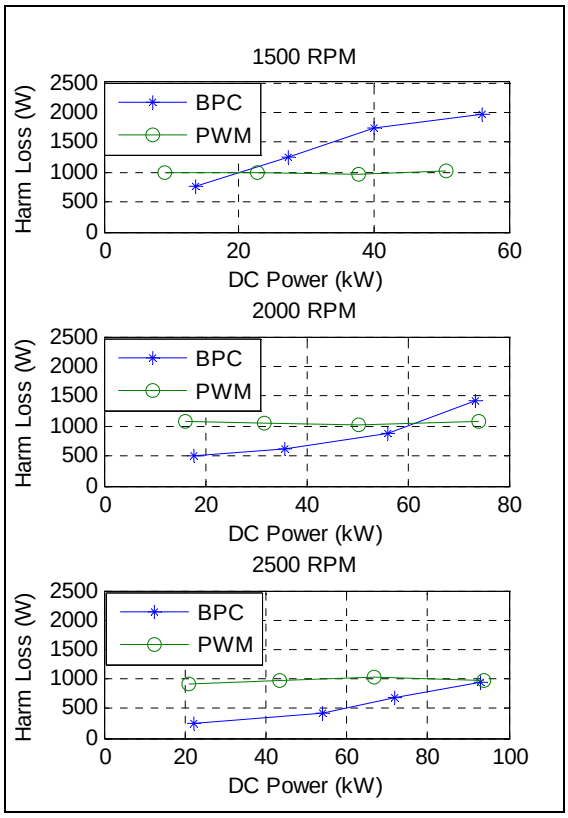

Figure 20. Harm Loss Plots.

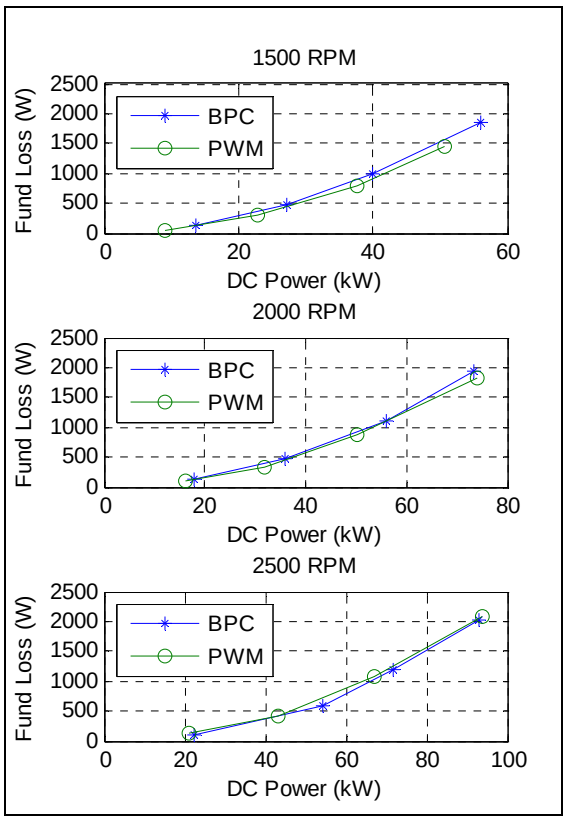

Figure 19. Fund Loss Plots.

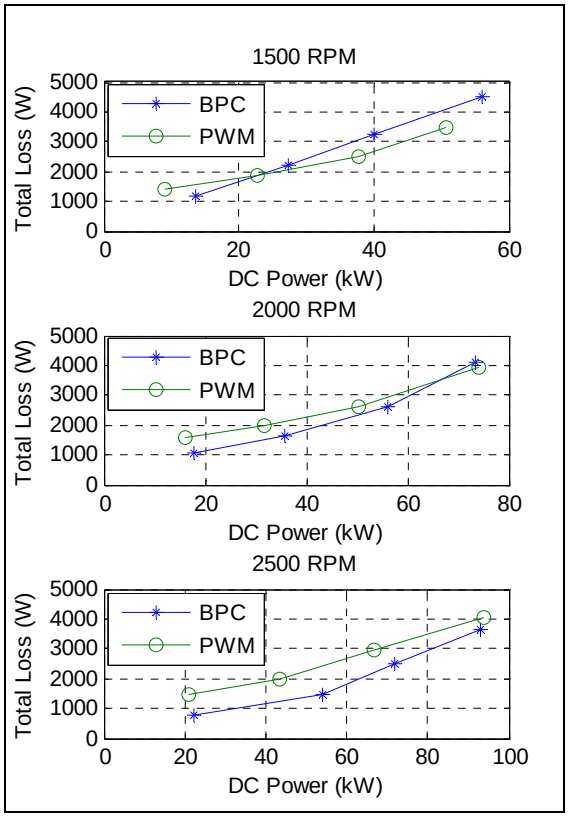

Figure 21. Total Loss Plots.

6 Conclusions

The feasibility of utilizing boost phase control to perform field oriented control to regulate the power flow for permanent magnet machines using standard hard switched PWM hardware to a DC bus has been demonstrated. Boost phase control only gates each of the 6 IGBTs one time each electrical cycle for a fraction of the electrical cycle thus the inverter 'switching' frequency is the same as the fundamental of the electric machine. For this paper, only generation power flow was demonstrated, but this is not a requirement of the algorithm, but rather a limitation of the hardware which was readily available to test which was an engine/generator. What was generally seen is that the losses in the inverter are generally lower using BPC than using PWM at 5 kHz switching frequency. As the PWM switching frequency increases, this benefit of lower losses in the inverter should increase. It was observed that the harmonic generator losses with PWM were relatively constant over both speed and power levels. For BPC as the speed increased the harmonic losses decreased and as the power for a given speed increased these harmonic losses increased. For all but the lowest speeds tested, BPC had lower or practically identical overall losses as compared to PWM.

7 Path Forward

Additional testing is planned for both higher speed (requiring flux weakening for both PWM and BPC) and also at other PWM switching frequencies to extend the comparisons.

Authors

John Kajs is working in developing hybrid electric power technologies primarily for the US Army. He holds B.S. and M.S. degrees in Electrical Engineering from the University of Texas at Austin.

Dr. Peter Mongeau is the technical director for Vestas Power Systems, before which he served as a founder and Technology VP for EML Research, Kaman Electromagnetics and DRS Electric Power Technologies. Dr. Mongeau earned his B.S and PhD in Physics from M.I.T. He has published over 30 technical papers and holds 11 U. S. Patents in the fields of machine design, power electronics and advanced controls. His specialty is the design and development of advanced electric machines and has served as the lead electric machine designer for numerous PM motors, generators and pulsed power machines.

Dr. Terence Burke is a member of the TARDEC Mobility/Hybrid Electric Research Team. He received his Ph.D. in Electrical Engineering from Rutgers University.
His experience includes combat hybrid-electric vehicle power systems and pulsed power, with an emphasis on wide bandgap power semiconductors, power conversion, and thermal management.

Ghassan (Gus) Khalil is the leader for the US Army Vehicle Power and Mobility Group.

BYRON WONG is an engineer with the U.S. Army RDECOM-TARDEC Ground Vehicle Power and Mobility Group. He is a member of the Hybrid Electric Research Team. He holds a B.S. in Electrical/Computer Engineering from Wayne State University as well as an M.B.A. from Walsh College.